

**Strength and reliability of WC-Co cemented carbides: Understanding
microstructural effects on the basis of R-curve behavior and
fractography**

J. M. Tarragó^{1,2,ϕ}, D. Coureaux^{1,3}, Y. Torres⁴, E. Jiménez-Piqué^{1,2}, L.
Schneider⁵, J. Fair⁶ and L. Llanes^{1,2}

¹CIEFMA, Department of Materials Science and Metallurgical Engineering, EEBE, Universitat Politècnica de Catalunya, 08019 Barcelona, Spain

²Barcelona Research Center in Multiscale Science and Engineering, Universitat Politècnica de Catalunya, 08019 Barcelona, Spain

³Facultad de Ingeniería Mecánica, Universidad de Oriente, 90500 Santiago de Cuba, Cuba.

⁴Departamento de Ingeniería y Ciencia de los Materiales y del Transporte, Universidad de Sevilla, 41092 Sevilla, Spain

⁵Sandvik Machining Solutions, Coventry CV4 0XG, UK

⁶Sandvik Hyperion, Coventry CV4 0XG, UK

^ϕ Current address: Sandvik Hyperion, 08107 Martorelles, Spain

Abstract

Strength and reliability of WC-Co cemented carbides (hardmetals) are dependent on effective fracture toughness as well as on nature, size and distribution of processing flaws. Regarding toughness, they exhibit a crack growth resistance (R-curve) behavior, derived from the development of a multiligament bridging zone at the crack wake. Accordingly, successful implementation of fracture mechanics requires consideration of tangency criterion, between applied stress intensity factor and R-curve, in addition to fractographic inspection. It is the aim of this study to evaluate the strength behavior of a series of experimental WC-Co grades on the basis of R-curve failure criteria. Results indicate that microstructural effects on the strength of hardmetals may be satisfactorily rationalized following the referred criterion. The analysis includes consideration of nature and distribution of fracture origins, found to be more diverse and wider respectively for the harder fine-grained grades. This experimental evidence, together with the fact that these hardmetals exhibit steeper rising R-curves than tougher coarse-grained ones, leads to lower reliability for the former. This investigation documents and validates the great relevance of R-curve behavior for optimizing the mechanical performance of WC-Co cemented carbides on the basis of microstructural design.

Keywords

WC-Co cemented carbides, strength, reliability, fractography, R-curve behavior

Introduction

Brittle fracture is one of the most common failure mechanisms in the application of cemented carbides as forming tools and structural components, particularly under the combined action of mechanical and contact loads [1]. In a large number of cases fracture stems from the propagation of pre-existing flaws either intrinsic to the manufacturing and/or post-treatment processes (e.g. Ref. [2–6]) or induced under service conditions (e.g. Refs. [7–9]). Similar to other brittle materials, tensile strength of cemented carbides depends on the size of the major flaw and exhibits wide scatter due to the variability associated with defect distribution. Accordingly, strength is size-dependent as the probability of finding a major flaw increases with specimen size. Within this context, Weibull statistics [10] have been frequently recalled as a suitable approach to rationalize the rupture strength and reliability of hardmetals (e.g. Refs. [11,12]).

An extensive number of studies have been devoted to analyze the influence of the microstructure on the fracture strength of hardmetals (e.g. Ref. [1,4,13–18]). Gurland and Bardzil documented that the strength initially increases with the binder mean free path (λ_{Co}) until it reaches a maximum at λ_{Co} values around 0.3-0.6 μm , and then it starts decreasing [13]. This behavior was associated with a brittle-ductile transition. For small λ_{Co} values, fracture mechanisms are governed by the brittle fracture of the WC continuous phase. Therefore, the decrease of the flexural strength with decreasing λ_{Co} was related to larger WC amounts and to higher contiguity values of the carbide phase. On the opposite side of the curve, the strength was dominated by the extensive plastic deformation of the binder phase. Thus, fracture strength was inversely proportional to λ_{Co} due to a decrease of the constraint degree exerted by the carbide phase on the binder, when increasing λ_{Co} value. This microstructure-strength perspective was shared by Fang [17], who plotted fracture strength against hardness and documented that the former goes through a peak at intermediate values of the latter. In line with Gurland's earlier discussion, Fang postulates that strength of hardmetals is based on the competitive action played between hardness and fracture toughness. However, Gurland's theory could not explain the high fracture strength dispersion measured in cemented carbides. This perception changed with the implementation of linear elastic fracture mechanics (LEFM) to rationalize the brittle behavior of hardmetals [2,3,14]. Within this

context, the fracture toughness is the material property that, combined with the critical pre-existing flaw sizes and the applied stress, determines the fracture strength of cemented carbides.

LEFM approach considers a fully brittle behavior with a failure process given by extension of critical flaws, without stable subcritical growth before fracture [1]. However, as widely reported in literature, cemented carbides exhibit subcritical crack growth under monotonic loads. It yields (and results from) the development of a crack-bridging multiligament mechanism at the crack wake [19,20]. This mechanism entails the development of a rising crack growth resistance curve [21]. The authors of this paper recently reported a relevant influence of microstructure on the R-curve characteristics of hardmetals [22]. It is the purpose of this investigation to evaluate the microstructure-strength relations for a series of experimental WC-Co grades on the basis of R-curve failure criteria. In doing so, special attention is paid to explaining the impact of R-curve behavior on the strength and reliability of cemented carbides.

Materials and experimental aspects

The investigated materials were a set of experimental WC-Co cemented carbide grades supplied by Sandvik Hyperion. Eight grades corresponding to different combinations of binder content and carbide mean grain size were studied. Specimen codes and key microstructural parameters - binder content ($V_{wt\%}$), mean grain size (d_{WC}), carbide contiguity (C_{WC}), and binder mean free path (λ_{Co}) - are listed in **Table I**. In the finer grades, concretely 3UF, 6UF, 10UF, 11M and 15UF, a small amount of Cr_3C_2 was added as grain growth inhibitor. Mean grain size was measured following the linear intercept method, using field emission scanning electron microscopy (FE-SEM) micrographs taken in a JEOL-7001F unit. Carbide contiguity and binder mean free path were deduced according to empirical relations from open literature [5,23,24].

Mechanical characterization includes hardness ($HV30$), flexural strength (σ_R) and fracture toughness (K_{Ic}). Hardness was measured using a Vickers diamond pyramidal indenter and applying a load of 294N.

In all the others cases, testing was conducted using a four-point bending fully articulated test jig with inner and outer spans of 20 and 40 mm, respectively. Flexural strength tests were performed on an Instron 8511 servohydraulic machine, and 10 to 15 specimens of 45x4x3 mm³ were tested per grade. The surface subjected to the maximum tensile loads was polished to mirror-like finish and the edges were chamfered to reduce their effect as stress raisers. Flexural strength results were analyzed using Weibull statistics. Fracture toughness was determined using 45x10x5 mm³ single edge pre-cracked beam (SEPB) specimens, with a notch length-to-specimen width ratio of 0.3, following the procedure proposed by Torres *et al.* [25]. A detailed fractographic analysis on broken specimens was carried out by means of FE-SEM in order to detect critical flaws that promoted failure. Subsequently, the size of identified critical flaws was measured using the image analysis free-available software ImajeJ.

Results and discussion

Influence of the microstructure on the flexural strength

Hardness, fracture toughness, fracture strength and Weibull characteristic strength (σ_0) and modulus (m) values for the investigated cemented carbides are given in **Table II**. The Weibull plots for studied materials are shown in **Fig. 1**. Very interesting, the harder grades (i.e. 3UF, 6UF and 10UF) exhibit a bi-modal strength distribution. Therefore, the Weibull modulus for these grades is not reported. On the other hand, the other materials exhibit a clearly uni-modal distribution. A fractographic analysis by means of FESEM was conducted in order to identify the critical flaws that promoted failure. Some examples of the different types of critical flaws evidenced for studied hardmetals are shown in **Fig. 2**. The larger scatter measured for the harder grades can be directly associated with two different defect populations, consisting of pores and inclusions for the low strength values, and abnormal coarse WC grains for the top part of the Weibull distribution. It is also interesting to point out that the higher strength determined values correspond to the specimens with the smaller defect sizes, in line with the theoretical framework established by LFM [3,26]. In addition, gathered information from **Fig. 1 and 2** indicates that under the consideration of defects of different nature but similar equivalent size, defects such as pores,

agglomerates or inclusions, imply a greater severity than intrinsic microstructural heterogeneities (i.e. abnormal coarse grains). This is in agreement with ideas given in literature for other ceramic materials [27]. Furthermore, if the Weibull analysis for 6UF grade is performed uniquely in the specimens fracturing from microstructural heterogeneities (i.e. the upper part of the Weibull distribution), the Weibull modulus would rise from 7 up to 23. This is a clear indication that an exhaustive control of critical flaws nature results in relevant strength and reliability enhancements in cemented carbides. On the other hand, critical defect population for the tougher grades is characterized by an absence of pores and inclusions, together with a tendency to simply consist on microstructural heterogeneities such as abnormally coarse WC particles.

In **Fig. 3**, fracture strength is plotted as a function of binder mean free path. In accordance with previous investigations [13,28], flexural strength increases with λ_{Co} until it reaches a maximum at values around $0.25 \mu\text{m}$ and then it decreases for larger λ_{Co} values. It can therefore be concluded that the material with the highest strength is neither the toughest nor the hardest, concepts that tend to merge in industrial areas. Therefore, a compromise between fracture toughness and hardness is required to achieve an optimum performance of the material.

It is also interesting to remark that strength dispersion evidenced for investigated cemented carbides grades with λ_{Co} over $0.25 \mu\text{m}$ is significantly lower than that observed for grades with smaller binder mean free paths. Two main factors may explain this significant difference in strength scatter. First, as previously indicated, and probably the main reason, the Weibull curve for the studied hardmetals with a short λ_{Co} exhibit a bi-modal behavior (**Fig. 1**). Meanwhile Weibull plots for the other studied hardmetals are clearly uni-modal. Second, as previously commented in the introduction, cemented carbides exhibit a rising crack growth resistance behavior that imparts reliability and damage tolerance to hardmetals tools and components [29–32]. The effective reliability enhancement derived from the crack bridging mechanism is a function of both fracture toughness and fracture strength of the composite material [22]. Strength reliability increases with the microstructural size, defined as $d_{WC} + \lambda_{Co}$, until it reaches a plateau

for $d_{WC} + \lambda_{Co}$ lengths of around 1 μm [22]. Consequently, it is reasonable to expect lower Weibull modulus for hardmetals with short binder mean paths than for coarser materials.

Estimation of the critical flaw size

The critical flaw sizes for investigated materials were estimated according to LEFM and R-curve tangency criteria by assuming them to be internal circular flaws (for embedded circular cracks, Y has a value of 1.12 [33]). On the one hand, LEFM failure criterion relates the fracture strength (σ_R) with the critical flaw size (a_{cr}) according to the expression [34]:

$$K_{Ic} = Y\sigma_R\sqrt{a_{cr}} \quad (1)$$

where Y is an un-dimensional crack geometric factor. On the other hand, when considering an R-curve behavior, the tangency criteria for unstable crack propagation prevails. This criteria defines that the material catastrophically fails when the following two conditions are satisfied [32]:

$$K_{app} = K_R \quad (2)$$

$$\frac{dK_{app}}{da} = \frac{dK_R}{da} \quad (4)$$

where K_{app} is the applied stress intensity factor, K_R is the crack-tip resistance stress intensity factor and a is the crack length. K_{app} and a may be related to the applied strength (σ_{app}) according to LEFM basic equation [34]:

$$K_{app} = Y\sigma_{app}\sqrt{a} \quad (3)$$

The crack growth resistance curve for investigated hardmetals can be estimated from an equation recently published by the authors to describe R-curve behavior of cemented carbides [21,22]:

$$K_R = K_{Ic} - (K_{Ic} - K_t)\exp\left[-\frac{\Delta a}{t}\right] \quad (4)$$

where K_t is the critical crack-tip stress intensity factor required for crack initiation, Δa is the subcritical crack growth length and t is a crack length normalizing parameter. Therefore, in accordance with instability criterion for R-curve materials, the size of the critical flaws can be determined as follows:

$$a_{cr} = \left(\frac{K_{eff}}{Y\sigma_R} \right)^2 - \Delta a \quad (5)$$

According to tangency criterion, rising R-curve materials fracturing from the propagation of “short” cracks are not able to develop the whole toughening capability, and fracture at effective toughness levels (K_{eff}) lower than the intrinsic fracture toughness measured for long cracks [21,22,32,35,36]. Furthermore, R-curve materials also exhibit stable subcritical crack growth extension before catastrophic failure. Reached effective toughness levels and subcritical crack growth lengths can be determined according to tangency criterion and they are a function of both R-curve shape and initial flaw [32,36]. This process is exemplified in **Fig. 4** for the 6UF and 15C investigated cemented carbides.

The area of the identified defects during the fractographic analysis was experimentally measured and compared to the estimated ones. In doing so, defects were considered to be circular shaped and therefore, an equivalent critical radius (a_{cr}) is reported. Critical flaw sizes experimentally measured and estimated using the LEFM (full black squares) and tangency (white circles) criteria are plotted in **Fig. 5** against the binder mean free path. Note that in the case of the experimentally measured critical defect sizes, a length range is given where the bottom and top values correspond to the smaller and larger identified flaws, respectively. No defects were identified during the fractographic examination for the hardmetal grade with the longest binder mean free path (22M) and consequently they are not shown in the graph. Absolute differences between the estimated flaw sizes estimated following the LEFM and the tangency failure criteria are rather small for the harder grades, but they are fairly large for the tougher cemented carbides and increasing with binder mean free path.

As it is clearly shown in **Fig. 5**, a really good agreement between the critical defect sizes experimentally measured and those estimated following LEFM and R-curve approaches is attained for the harder grades, even though obtained $a_{cr,R-curve}$ lengths are slightly lower. However, for the tougher grades,

estimated $a_{cr,R-curve}$ values clearly match with the sizes experimentally measured in the identified critical flaws, whereas the application of the LEFM theory results in a flaw size overestimation. This fact reflects the need of taking into consideration the subcritical crack growth extension and the effective developed toughness for rationalizing the fracture behavior of cemented carbides [22]. On the one hand, low K_{eff} values imply larger estimated size differences between both criteria. On the other hand, large subcritical crack growth values lead to an overestimation of critical flaw sizes by LEFM.

Microstructural effects on failure probability

As previously commented, the fracture behavior of cemented carbides is of stochastic nature [2–4,11,12,14]. Therefore, probabilistic failure mechanics are essential for proper designing with this brittle-like material [37,38]. According to Weibull distribution standards [39], the range of failure probabilities covered by the experimental assessment of the Weibull curve increases with the dimension of the sample (i.e. the number of tested specimens). However, due to the costs of the specimens the number of tested specimens is usually rather small [40]. In this investigation, the sample size was limited between 10 to 15 specimens, and therefore the range of considered probabilities of failure was kept from a 5% to a 95%. Nevertheless, for designing purposes of tools and components, the measured characteristic strength usually needs to be extrapolated to really low probabilities of failure and to different effective loaded volumes [40]. In cemented carbides this extrapolation is not straightforward, as they exhibit a R-curve behavior that may imply a deviation from Weibull statistics [11,22,40]. Moreover, it has been observed in this investigation, in some cases the fracture of cemented carbides exhibit a multi-modal flaw population where a Weibull distribution is not expected to occur [40]. Therefore, a deep knowledge of the fracture process of cemented carbides is demanded for the proper design of heavily stressed tools and components.

According to Weibull theory [10,41], the strength of an individual specimen (σ_i) of a sample can be deduced for a given failure probability (P_i) by using the following equation:

$$\sigma_i = \sigma_0 \left[\ln \left(\frac{1}{1-P_f} \right) \right]^{1/m} \quad (6)$$

Then, by experimentally determining σ_0 and m , the fracture strength for each failure probability can be estimated.

Fracture strength corresponding to a fixed failure probability level was estimated from Eq. (6) for the investigated cemented carbide grades and plotted against the fracture toughness. This process was iterated for a probability of failure range going from 5% to a 95%, and by selecting a 5% span between P_f values. As an outcome of this exercise, a fracture strength contour plot with fracture toughness in the coordinate axis and failure probability in the ordinate one was drawn (**Fig. 6**). This graph can be divided in three areas corresponding to low-, medium- and, high-toughness grades. Several interesting observations may be done. First, hardmetals with low fracture toughness levels exhibit relatively high fracture strength values at large failure probabilities. However, strength levels decrease rapidly as failure probability decreases. This large scatter in strength is related to its low reliability caused by the corresponding bi-modal Weibull distribution and by having an R-curve behaviour with a small increase. Their rather high strength levels for medium failure probabilities are probably a consequence of having a high hardness [17] and a highly constrained binder phase [13]. Furthermore, rather small defects sizes were identified for these grades. Second, cemented carbides with medium fracture toughness levels (K_{Ic} from 10–13 $\text{MPa}\sqrt{\text{m}}$) exhibit the larger fracture strength levels for all the range of failure probabilities. Their high reliability accounts for having narrow defect sizes distributions and for exhibiting medium rising crack growth resistance behaviour [22]. Third, the tougher grades exhibit quite small strengths. The lower strength levels measured for these materials can be attributed to the high plasticity and low hardness levels of those grades, together with the fact of having defect populations consisting of large-sized flaws. On the other hand, their extremely high Weibull modulus is principally related to their high toughness level, which imparts extremely high damage tolerance levels [22,42,43].

Conclusions

The influence of the microstructure on the fracture strength and reliability of cemented carbides was investigated. In doing so, the microstructure-strength relations for the studied materials were discussed on the basis of the tangency criterion for R-curve materials. Based on obtained results the following conclusions may be drawn:

1. The investigated hardmetals with lower binder mean free path (i.e. with the higher hardness value) exhibit a wide range of fracture origin types. Consequently, they show a bi-modal Weibull distribution that strongly affects its reliability. This fact is aggravated by the short and steep R-curve exhibited by these materials, owing to its low fracture toughness. On the other hand, studied grades with medium- and high- toughness levels had extremely high reliabilities associated with defect types that mainly consist of microstructural heterogeneities, in addition to their longer and less steep R-curve behaviors.
2. The implementation of the LEFM framework for rationalizing the fracture behavior of cemented carbides was validated for hardmetals grades with low binder mean free paths. However, this theoretical approach is not valid to describe the fracture behavior of tougher grades and results in an overestimation of critical defect sizes. This fact arises from the requirement of considering the influence of the R-curve behavior of hardmetals for the assessment of their fracture strength. Consequently, the critical flaw sizes estimated according to tangency criteria for R-curve materials strongly agree with those experimentally measured from the defects identified during the fractographic analysis.
3. The relation of fracture strength with fracture toughness may be divided in three zones. The first, corresponding to the harder cemented carbides, is characterized by exhibiting a wide range of strength levels for different failure probabilities; and therefore, low strength reliabilities. In the second one, comprised by hardmetals with intermediate toughness levels, the strength reach

their maximum values, combined with an extremely high reliability. The third zone is given by the tougher grades that exhibit lower strength values but extremely high reliabilities (and outstanding damage tolerance).

Acknowledgements

This work was financially supported by the Spanish Ministerio de Economía y Competitividad through Grant MAT2015-70780-C4-3-P (MINECO/FEDER). Funding of this investigation was also supplied by the Andalusian government (Spain) under the excellence project P12-TEP-2622. Additionally, J.M. Tarragó and D. Coureaux acknowledge the Ph.D. scholarships received from the collaborative Industry-University program between Sandvik Hyperion and Universitat Politècnica de Catalunya and from the Agencia Española de Cooperación Internacional (MAEC-AECID), respectively.

References

- [1] A.V. Shatov, S.S. Ponomarev, S.A. Firstov, Fracture and strength of hardmetals at room temperature, in: V.K. Sarin, D. Mari, L. Llanes (Eds.), *Comprehensive Hard Materials*, Elsevier, UK, 2014: pp. 301–343.
- [2] P. Kenny, The application of fracture mechanics to cemented tungsten carbides, *Powder Metall.* 14 (1971) 22–38.
- [3] H. Suzuki, K. Hayashi, The strength of WC–Co cemented carbide in relation to structural defects, *Trans. Japan Inst. Met.* 16 (1975) 353–360.
- [4] E.A. Almond, B. Roebuck, Defect-initiated fracture and the bend strength of WC–Co hardmetals, *Met. Sci.* 11 (1977) 458–461.
- [5] B. Roebuck, E.A. Almond, Deformation and fracture processes and the physical metallurgy of WC–Co hardmetals, *Int. Mater. Rev.* 33 (1988) 90–110.

- [6] B. Casas, Y. Torres, L. Llanes, Fracture and fatigue behavior of electrical-discharge machined cemented carbides, *Int. J. Refract. Met. Hard Mater.* 24 (2006) 162–167.
- [7] B. Casas, X. Ramis, M. Anglada, J.M. Salla, L. Llanes, Oxidation-induced strength degradation of WC–Co hardmetals, *Int. J. Refract. Met. Hard Mater.* 19 (2001) 6–12.
- [8] V.A. Pugsley, G. Korn, S. Luyckx, H.G. Sockel, W. Heinrich, M. Wolf, H. Feld, R. Schulte, The influence of a corrosive wood-cutting environment on the mechanical properties of hardmetal tools, *Int. J. Refract. Met. Hard Mater.* 19 (2001) 311–318.
- [9] J.M. Tarragó, G. Fargas, E. Jimenez-Piqué, A. Felip, L. Isern, D. Coureaux, J.J. Roa, I. Al-Dawery, J. Fair, L. Llanes, Corrosion damage in WC–Co cemented carbides: residual strength assessment and 3D FIB-FESEM tomography characterisation, *Powder Metall.* 57 (2014) 324–330.
- [10] W. Weibull, A statistical distribution function of wide applicability, *J. Appl. Mech.* 18 (1951) 293–297.
- [11] T. Klünsner, S. Wurster, P. Supancic, R. Ebner, M. Jenko, J. Glätzle, A. Püschel, R. Pippan, Effect of specimen size on the tensile strength of WC–Co hard metal, *Acta Mater.* 59 (2011) 4244–4252.
- [12] Y. Torres, R. Bermejo, F.J. Gotor, E. Chicardi, L. Llanes, Analysis on the mechanical strength of WC-Co cemented carbides under uniaxial and biaxial bending, *Mater. Des.* 55 (2014) 851–856.
- [13] J. Gurland, P. Bardzil, Relation of strength, composition, and grain size of sintered WC-Co alloys, *J. Met.* 7 (1955) 311–315.
- [14] H.F. Fischmeister, Development and present status of the science and technology of hard materials, in: R.K. Viswanatham, D.J. Rowcliffe, J. Gurland (Eds.), *Proceedings of the 1st International Conference on Science of Hard Materials*, Plenum Press, New York, 1983: pp. 1–45.

- [15] E.A. Almond, Deformation characteristics and mechanical properties of hardmetals, in: R.K. Viswanadham, D. Rowcliffe, J. Gurland (Eds.), Proceedings of the 1st International Conference on Science of Hard Materials, Plenum Press, New York, 1983: pp. 517–561.
- [16] F. Osterstock, J.L. Chermant, Some aspects of the fracture of WC–Co composites, in: R.K. Viswanadham, D. Rowcliffe, J. Gurland (Eds.), Proceedings of the 1st International Conference on Science of Hard Materials, Plenum Press, New York, 1983: pp. 615–629.
- [17] Z. Zak Fang, Correlation of transverse rupture strength of WC–Co with hardness, *Int. J. Refract. Met. Hard Mater.* 23 (2005) 119–127.
- [18] A.V. Shatov, S.S. Ponomarev, S.A. Firstov, Fracture of WC–Ni cemented carbides with different shape of WC crystals, *Int. J. Refract. Met. Hard Mater.* 26 (2008) 68–76.
- [19] L.S. Sigl, H.E. Exner, Experimental study of the mechanics of fracture in WC–Co alloys, *Metall. Trans. A.* 18A (1987) 1299–1308.
- [20] L.S. Sigl, H.F. Fischmeister, On the fracture toughness of cemented carbides, *Acta Metall.* 36 (1988) 887–897.
- [21] J.M. Tarragó, E. Jiménez-Piqué, L. Schneider, D. Casellas, Y. Torres, L. Llanes, FIB/FESEM experimental and analytical assessment of R-curve behavior of WC-Co cemented carbides, *Mater. Sci. Eng. A.* 645 (2015) 142–149.
- [22] J.M. Tarragó, D. Coureaux, Y. Torres, D. Casellas, I. Al-Dawery, L. Schneider, L. Llanes, Microstructural effects on the R-curve behavior of WC-Co cemented carbides, *Mater. Des.* 97 (2016) 492–501.
- [23] H.E. Exner, Physical and chemical nature of cemented carbides, *Int. Met. Rev.* 24 (1979) 149–173.

- [24] J.M. Tarragó, D. Coureaux, Y. Torres, F. Wu, I. Al-Dawery, L. Llanes, Implementation of an effective time-saving two-stage methodology for microstructural characterization of cemented carbides, *Int. J. Refract. Met. Hard Mater.* 55 (2016) 80–86.
- [25] Y. Torres, D. Casellas, M. Anglada, L. Llanes, Fracture toughness evaluation of hardmetals: influence of testing procedure, *Int. J. Refract. Met. Hard Mater.* 19 (2001) 27–34.
- [26] S.I. Cha, K.H. Lee, H.J. Ryu, S.H. Hong, Effect of size and location of spherical pores on transverse rupture strength of WC-Co cemented carbides, *Mater. Sci. Eng. A.* 486 (2008) 404–408.
- [27] J.P. Singh, Effect of flaws on the fracture behavior of structural ceramics: A review, *Adv. Ceram. Mater.* 3 (1988) 18–27.
- [28] J. Gurland, New scientific approaches to development of tool materials, *Int. Mater. Rev.* 33 (1988) 151–166.
- [29] P.A. Mataga, Deformation of crack-bridging ductile reinforcements in toughened brittle materials, *Acta Metall.* 37 (1989) 3349–3359.
- [30] Y. Torres, R. Bermejo, L. Llanes, M. Anglada, Influence of notch radius and R-curve behaviour on the fracture toughness evaluation of WC–Co cemented carbides, *Eng. Fract. Mech.* 75 (2008) 4422–4430.
- [31] Y. Torres, J.M. Tarrago, D. Coureaux, E. Tarrés, B. Roebuck, P. Chan, M. James, B. Liang, M. Tillman, R.K. Viswanadham, K.P. Mingard, A. Mestra, L. Llanes, Fracture and fatigue of rock bit cemented carbides: Mechanics and mechanisms of crack growth resistance under monotonic and cyclic loading, *Int. J. Refract. Met. Hard Mater.* 45 (2014) 179–188.
- [32] D. Munz, What can we learn from R-curve measurements?, *J. Am. Ceram. Soc.* 90 (2007) 1–15.
- [33] Y. Murakami, *Stress intensity factors handbook*, 3rd ed., Elsevier, Kyoto, 1999.

- [34] G.R. Irwin, Fracture, in: Handbuch Der Physics, Springer-Verlag, Berlin, 1958.
- [35] J.J. Kruzic, R.L. Satet, M.J. Hoffmann, R.M. Cannon, R.O. Ritchie, The utility of R-curves for understanding fracture toughness-strength relations in bridging ceramics, *J. Am. Ceram. Soc.* 91 (2008) 1986–1994.
- [36] M.E. Launey, R.O. Ritchie, On the fracture toughness of advanced materials, *Adv. Mater.* 21 (2009) 2103–2110.
- [37] D. Rubes, B. Smoljan, R. Danzer, Main features of designing with brittle materials, *J. Mater. Eng. Perform.* 12 (2003) 220–228.
- [38] R. Danzer, T. Lube, P. Supancic, R. Damani, Fracture of ceramics, *Adv. Eng. Mater.* 10 (2008) 275–298.
- [39] ASTM C 1239-00: Standard practice for reporting uniaxial strength data and estimating Weibull distribution parameters for advanced ceramics, USA, 2000.
- [40] R. Danzer, P. Supancic, J. Pascual, T. Lube, Fracture statistics of ceramics – Weibull statistics and deviations from Weibull statistics, *Eng. Fract. Mech.* 74 (2007) 2919–2932.
- [41] J.B. Wachtman, Mechanical properties of ceramics, 2nd ed., John Wiley & Sons, New York, 1996.
- [42] J.M. Tarragó, G. Fargas, L. Isern, S. Dorvlo, E. Tarres, C.M. Müller, E. Jiménez-Piqué, L. Llanes, Microstructural influence on tolerance to corrosion-induced damage in hardmetals, *Mater. Des.* 111 (2016) 36–43.
- [43] J.M. Tarragó, S. Dorvlo, J. Esteve, L. Llanes, Influence of the microstructure on the thermal shock behavior of cemented carbides, *Ceram. Int.* 42 (2016) 12701–12708.

List of tables

Table I. Microstructural parameters for investigated cemented carbides.

Table II. Hardness, flexural strength, Weibull characteristic strength, Weibull modulus and fracture toughness values for investigated cemented carbides.

ACCEPTED MANUSCRIPT

List of figures

Figure 1: Fracture strength values in the form of Weibull distribution for studied hardmetal grades. The investigated cemented carbide grades with the lower binder mean free path exhibits a: (a) bi-modal Weibull distribution, whereas the other grades have (b) uni-modal Weibull curves.

Figure 2: FESEM micrographs of failure initiation sites; namely: (a) carbide agglomerate in the 3UF grade, (b) pore in the 10UF grade, (c) abnormal coarse grain in the 10C grade and, (d) binderless agglomerate of coarse WC particles in the 15C grade.

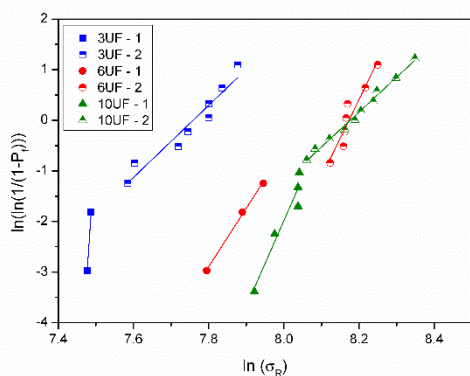
Figure 3: Fracture strength as a function of the binder mean free path.

Figure 4: Estimated crack resistance curves for the 6UF and 15C investigated hardmetals (full lines). Unstable criterion is reached when tangency conditions between the R-curve and the applied stress intensity factor (dash-dot lines) are fulfilled. Dashed lines indicate the subcritical crack growths lengths and effective toughness levels reached when tangency criteria is accomplished (i.e. unstable crack growth). Fracture is estimated for the experimentally measured flexural strength values of 3287MPa and 2570MPa for 6UF and 15C, respectively.

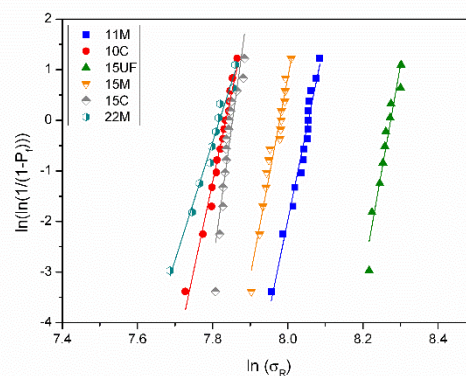
Figure 5: Estimated and experimentally determined critical flaws sizes.

Figure 6: Fracture strength as a function of fracture toughness (coordinate axis) and probability of failure (ordinate axis).

FIGURES



(a)



(b)

Figure 1: Fracture strength values in the form of Weibull distribution for studied hardmetal grades. The investigated cemented carbide with the lower binder mean free path (a) exhibits a bi-modal Weibull distribution whereas the other grades (b) have uni-modal Weibull curves.

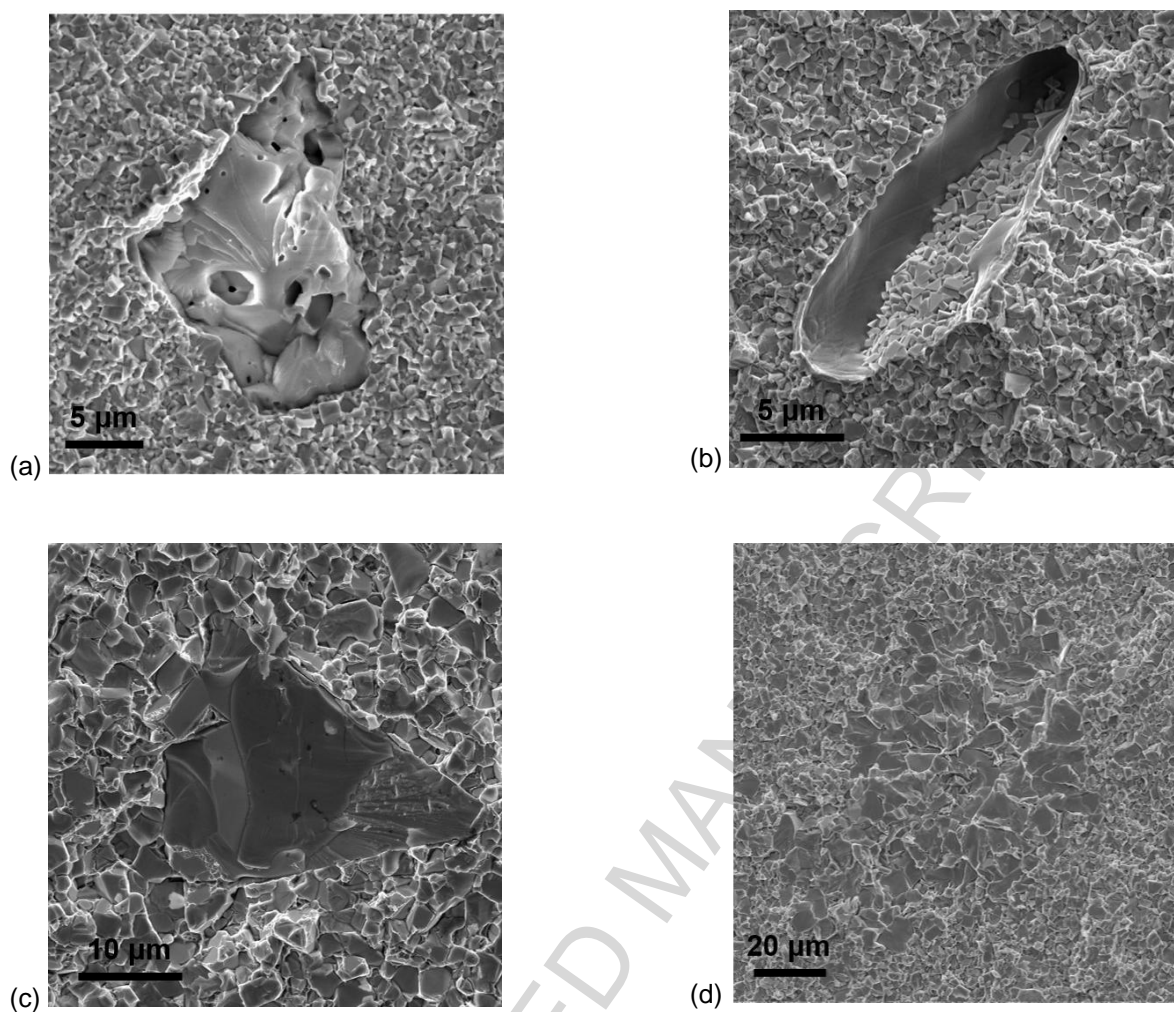


Figure 2: FESEM micrographs of failure initiation sites; namely: (a) carbide agglomerate in the 3UF grade, (b) pore in the 10UF grade, (c) abnormal coarse grain in the 10C grade and, (d) binderless agglomerate of coarse WC particles in the 15C grade.

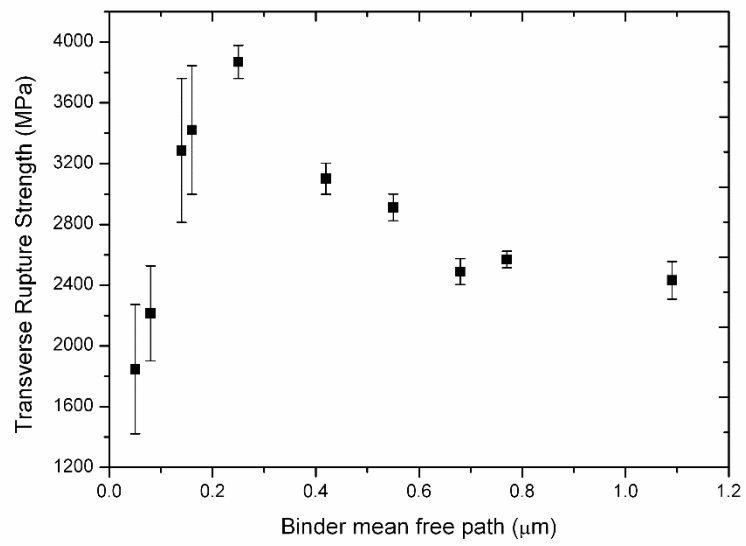


Figure 3: Fracture strength as a function of the binder mean free path.

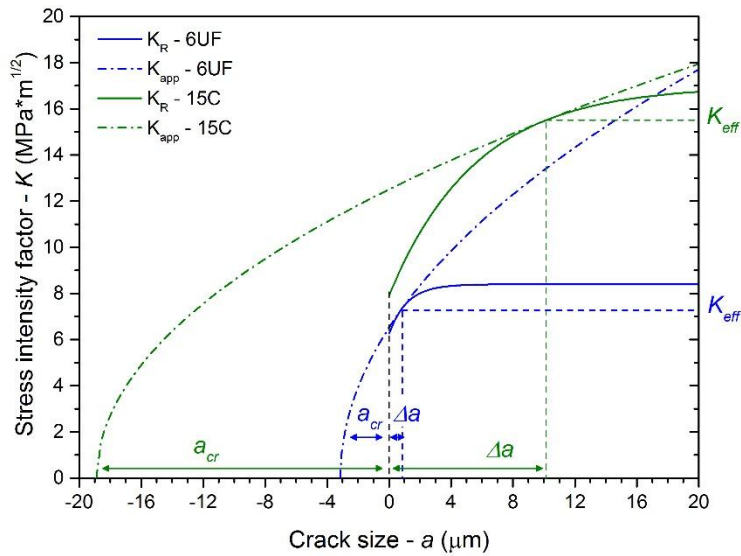


Figure 4: Estimated crack resistance curves for the 6UF and 15C investigated hardmetals (full lines). Unstable criterion is reached when tangency conditions between the R-curve and the applied stress intensity factor (dash-dot lines) are fulfilled. Dashed lines indicate the subcritical crack growths lengths and effective toughness levels reached when tangency criteria is accomplished (i.e. unstable crack growth). Fracture is estimated for the experimentally measured flexural strength values of 3287MPa and 2570MPa for 6UF and 15C, respectively.

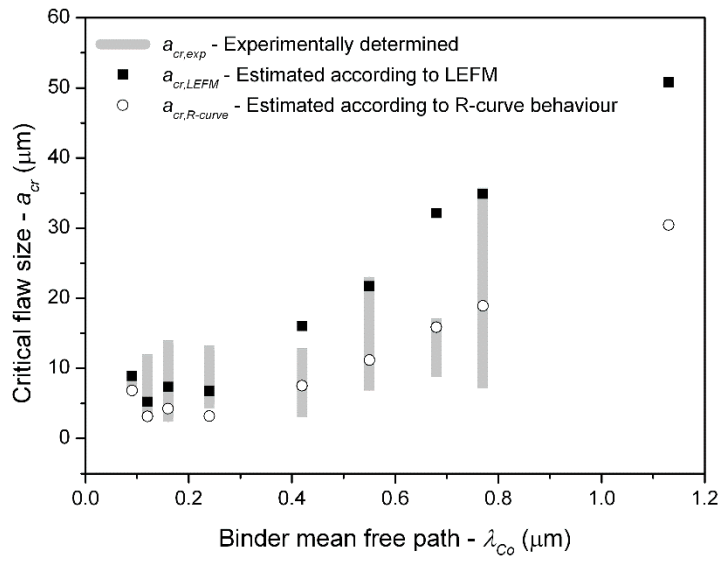


Figure 5: Estimated and experimentally determined critical flaws sizes.

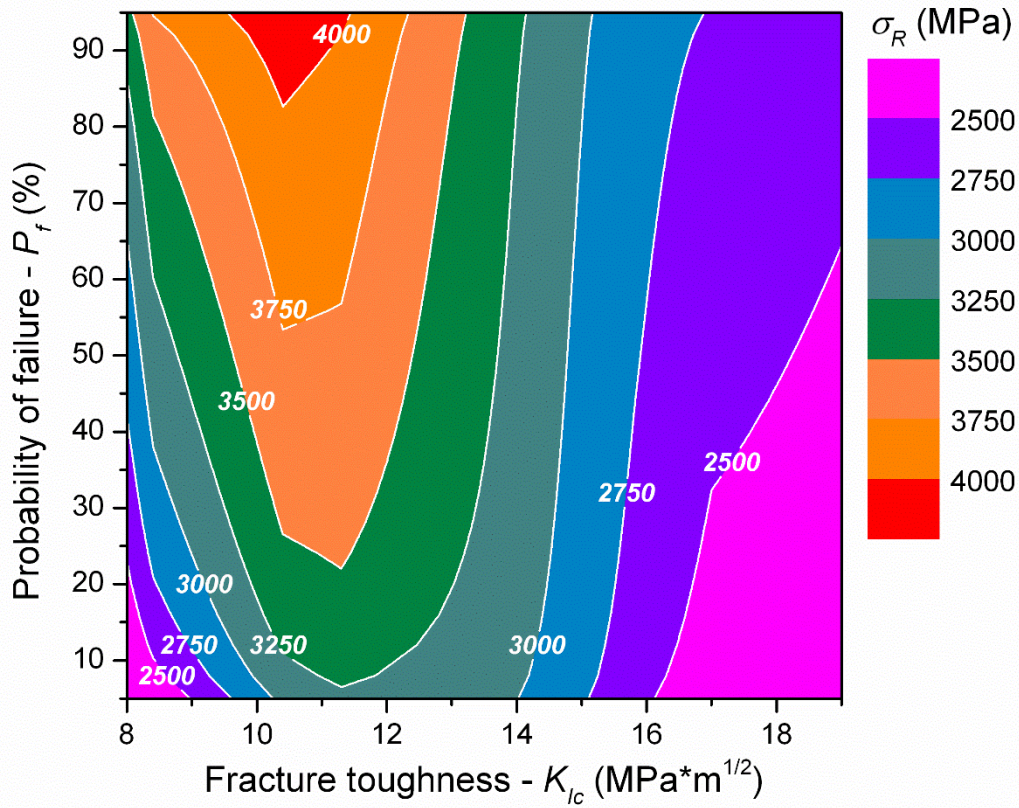


Figure 6: Fracture strength as a function of fracture toughness (coordinate axis) and probability of failure (ordinate axis).

TABLES

	$V_{wt. \%}$	d_{wc} (MPa)	C_{wc} (MPa)	λ_{Co} (μm)
3UF	3	0.37 ± 0.22	0.74 ± 0.42	0.09 ± 0.05
6UF	6	0.40 ± 0.21	0.61 ± 0.12	0.12 ± 0.06
10UF	10	0.39 ± 0.19	0.46 ± 0.06	0.16 ± 0.06
11M	11	1.12 ± 0.71	0.38 ± 0.07	0.42 ± 0.28
10C	10	2.33 ± 1.38	0.31 ± 0.11	0.68 ± 0.48
15UF	15	0.47 ± 0.22	0.36 ± 0.02	0.24 ± 0.11
15C	15	1.70 ± 1.08	0.27 ± 0.07	0.77 ± 0.54
22M	22	1.64 ± 0.75	0.19 ± 0.04	1.13 ± 0.56

Table I. Microstructural parameters for investigated cemented carbides.

	<i>HV30</i>	σ_R (MPa)	σ_0 (MPa)	<i>m</i>	K_{Ic} (MPa \sqrt{m})
3UF	18.9 ± 0.8	2214 ± 313	2351	-	7.4 ± 0.7
6UF	16.9 ± 0.2	3287 ± 473	3506	-	8.4 ± 0.3
10UF	15.7 ± 0.6	3422 ± 512	3598	-	10.4 ± 0.3
11M	12.8 ± 0.2	3101 ± 102	3149	36	13.9 ± 0.3
10C	11.4 ± 0.2	2489 ± 85	2522	35	15.8 ± 0.3
15UF	13.2 ± 0.1	3869 ± 109	3919	42	11.3 ± 0.6
15C	10.2 ± 0.1	2570 ± 54	2570	54	17.0 ± 0.2
22M	7.7 ± 0.1	2431 ± 124	2487	24	19.4 ± 1.4

Table II. Hardness, flexural strength, Weibull characteristic strength, Weibull modulus and fracture toughness values for investigated cemented carbides.

Highlights

- LEFM framework is valid to describe fracture behavior of low-toughness hardmetals
- Medium and high-toughness hardmetals require the consideration of R-curve behavior
- Low-toughness grades tend to exhibit medium strength levels and low reliabilities
- Medium-toughness hardmetals tend to exhibit large strength and reliability levels
- High-toughness grades tend to exhibit low strengths levels but high reliabilities